HHS Public Access

Author manuscript

Curr Biol. Author manuscript; available in PMC 2021 November 16.

Published in final edited form as:

Curr Biol. 2020 November 16; 30(22): 4510–4518.e6. doi:10.1016/j.cub.2020.08.069.

Ghrelin Signaling Affects Feeding Behavior, Metabolism, and Memory through the Vagus Nerve

Elizabeth A. Davis[1], **Hallie S. Wald**[2], **Andrea N. Suarez**[1], **Jasenka Zubcevic**[3], **Clarissa M. Liu**[4], **Alyssa M. Cortella**[1], **Anna K. Kamitakahara**[5], **Jaimie W. Polson**[6], **Myrtha Arnold**[7], **Harvey J. Grill**[2], **Guillaume de Lartigue**[8,9,*], **Scott E. Kanoski**[1,4,10,11,*]

[1]Department of Biological Sciences, Human and Evolutionary Biology Section, Dornsife College of Letters, Arts and Sciences, University of Southern California, Los Angeles, CA 90089, USA [2]Institute of Diabetes, Obesity and Metabolism, Graduate Groups of Psychology and Neuroscience, University of Pennsylvania, Philadelphia, PA 19104, USA [3]Department of Physiological Sciences, College of Veterinary Medicine, University of Florida, Gainesville, FL 32610, USA [4]Neuroscience Graduate Program, University of Southern California, Los Angeles, CA, USA [5]Children's Hospital of Los Angeles, Los Angeles, CA 90089, USA [6]School of Medical Sciences & Bosch Institute, The University of Sydney, Sydney 2006, Australia [7]Department of Health Sciences and Technology, ETH Zurich, Zurich 8092, Switzerland [8]Pharmacodynamics Department, College of Pharmacy, University of Florida, Gainesville, FL 32610, USA [9]Center for Integrative Cardiovascular and Metabolic Disease, University of Florida, Gainesville, FL 32610, USA [10]Twitter: @Kanoski_Lab [11]Lead Contact

SUMMARY

Vagal afferent neuron (VAN) signaling sends information from the gut to the brain and is fundamental in the control of feeding behavior and metabolism [1]. Recent findings reveal that VAN signaling also plays a critical role in cognitive processes, including affective motivational behaviors and hippocampus (HPC)-dependent memory [2–5]. VANs, located in nodose ganglia, express receptors for various gut-derived peptide signals; however, the function of these receptors with regard to feeding behavior, metabolism, and memory control is poorly understood. We hypothesized that VAN-mediated processes are influenced by ghrelin, a stomach-derived orexigenic hormone, via communication to its receptor (GHSR) expressed on gut-innervating VANs. To examine this hypothesis, rats received nodose ganglia injections of an adeno-associated virus (AAV) expressing short hairpin RNAs targeting GHSR (or a control AAV) for RNAi-

*Correspondence: gdelartigue@ufl.edu (G.d.L.), kanoski@usc.edu (S.E.K.).

AUTHOR CONTRIBUTIONS

S.E.K., G.d.L., E.A.D., H.J.G., H.S.W., and J.Z. designed experiments; G.D. and M.A. performed nodose injection procedures; E.A.D., A.N., and H.S.W. assisted with nodose injection procedures; A.N. performed vagotomies; J.Z. and J.W.P. performed DAPR; E.A.D., H.S.W., A.N., and C.M.L. performed behavioral experiments; E.A.D., A.K.K., A.N.S., H.S.W., J.Z., and J.W.P. harvested tissues; E.A.D. performed gene expression experiments; A.M.C. and E.A.D. performed immunoblotting experiments; A.M.C. performed FISH experiments; E.A.D., J.Z., G.D., H.S.W., and S.E.K. analyzed the data; E.A.D. drafted the manuscript; A.M.C. provided the figure art; S.E.K. edited the manuscript; and all authors reviewed and approved of the manuscript.

SUPPLEMENTAL INFORMATION

Supplemental Information can be found online at https://doi.org/10.1016/j.cub.2020.08.069.

DECLARATION OF INTERESTS

The authors declare no competing interests.

mediated VAN-specific GHSR knockdown. Results reveal that VAN GHSR knockdown induced various feeding and metabolic disturbances, including increased meal frequency, impaired glucose tolerance, delayed gastric emptying, and increased body weight compared to controls. Additionally, VAN-specific GHSR knockdown impaired HPC-dependent contextual episodic memory and reduced HPC brain-derived neurotrophic factor expression, but did not affect anxiety-like behavior or general activity levels. A functional role for endogenous VAN GHSR signaling was further confirmed by results revealing that VAN signaling is required for the hyperphagic effects of ghrelin administered at dark onset, and that gut-restricted ghrelin-induced increases in VAN firing rate require intact VAN GHSR expression. Collective results reveal that VAN GHSR signaling is required for both normal feeding and metabolic function as well as HPC-dependent memory.

In Brief

Davis et al. investigate the role of vagal afferent ghrelin signaling on memory, metabolism, and feeding behavior by using a viral strategy to selectively knock down ghrelin receptor (GHSR) in the vagus nerve. Results reveal various feeding and metabolic disturbances, as well as impaired hippocampal-dependent contextual episodic memory.

RESULTS

Nodose Ganglia *Ghsr* Is Expressed Exclusively in Neurons and at Similar Levels in Left and Right NG

Both rats and mice express *Ghsr* mRNA in the nodose ganglia (NG) [6–9]. qPCR analyses show that *Ghsr* expression did not differ between the left and the right NG in either the rat (Figure 1A) or the mouse (Figure 1B). While all subsequent results are from rats, mice are included in this experiment given a recent report that left versus right VAN signaling differ with regard to neuro-cognitive outcomes in mice [5].

Fluorescence *in situ* hybridization (FISH) analyses reveal that NG *Ghsr* mRNA is exclusively expressed in neurons, as evident from colocalization of *Ghsr* with the neuronal marker *NeuN*, with no *Ghsr* observed in cells absent of *NeuN* (Figure 1C). Quantitative analyses confirm that *Ghsr* is co-expressed in ~73% of *NeuN*+ VAN (SEM ± 7.6%).

Vagus Nerve Signaling Is Required for the Hyperphagic Effects of Peripheral Ghrelin during the Dark Cycle

We investigated whether the vagus nerve is functionally required for the orexigenic effects of peripheral ghrelin by comparing 2 h cumulative food intake following intraperitoneal (i.p.) ghrelin injections (0, 20, or 40 μg/kg bodyweight [BW]) at dark onset in rats that had subdiaphragmatic vagotomy (SDV) compared with sham surgery (Figure 1D). Results revealed that there was a main effect of surgery (Figure 1E; $p < 0.05$), and post hoc analyses revealed that 40 μg/kg ghrelin significantly increased food intake versus saline in the control group, but not in the SDV group (Figure 1E). The 20 μg/kg dose did not reach statistical significance for either group. These results indicate that the vagus nerve is required for the orexigenic effects of ghrelin when tested during the dark cycle. SDV animals weighed

significantly less than controls at the time of testing (sham, 409.8 ± 8.5 g; SDV, 362.6 ± 9.5 g; $p < 0.05$). However, food intake between groups in the saline condition was not significantly different when normalized per 100 g BW ($p > 0.05$; Figure S2A), suggesting that the lack of a ghrelin hyperphagic effect in the SDV group is unlikely based on a ceiling effect for maximal food intake.

VAN *Ghsr* Expression Is Reduced with Targeted RNAi without Affecting Expression of Other Feeding-Relevant Receptors

We developed an approach to knock down GHSR specifically within VAN. Bilateral NG injections of an AAV for *Ghsr*-targeted RNAi (AAV-2-GFP-rGHSR-shRNA) (Figure 1F) were administered, which yielded expression of the GFP transgene driven by the AAV (Figure 1G) and significantly reduced VAN *Ghsr* mRNA expression by ~86% compared with a control AAV (Figure 1H; $p < 0.05$). To evaluate potential compensatory changes in expression of other feeding-relevant VAN receptors previously shown to interact with VAN GHSR [6], we evaluated *Mch1r* and *Cb1r* mRNA expression in the NG of rats that received Ghsr short hairpin RNA (shRNA) versus controls. Results reveal no differences in *Mch1r* or *Cb1r* expression between groups (Figure S3), indicating that subsequent results are unlikely to be secondary to changes in VAN *Mch1r* or *Cb1r* signaling.

VAN Neural Responses to Gut-Restricted Ghrelin Require Intact VAN GHSR

To investigate whether GI-restricted ghrelin administration evokes VAN neural responses via GHSR, an *in situ* model of a decorticated artificially perfused rat (DAPR; Figure 2A) was used that allows for simultaneous recording of neural activity from both left (LNG) and right (RNG) NG in response to an intra-arterial injection of ghrelin (5 nmol versus saline) restricted to the GI tract. Representative traces show responses to ghrelin from an animal with GHSR knockdown in the RNG and control AAV in the LNG (Figure 2B), and vice versa (Figure 2C). When responses to ghrelin were compared between vagal recordings from the control-injected side, there were no differences between left and right responses (Figure 2D). However, when comparing the vagal response between the GHSR knockdown and the contralateral control AAV side within-animal, there was a statistically significant decrease in maximum response on the knockdown side (Figure 2E; $p < 0.05$). Vagal afferent activity in response to intra-arterial injection of cholecystokinin (CCK; 1 μg) was also measured (Figure 2G). CCK infusion yielded an increase in VAN neural activity in both control and knockdown sides, with a trend toward a greater response to CCK in the RNG versus LNG ($p = 0.09$; Figure 2H). However, there were no differences in neural response to CCK between knockdown and controls (Figure 2I). Given that ghrelin circulation was precluded from supradiaphragmatic access to GHSRs expressed in NG cell bodies, these results highlight a functional role for GHSRs likely expressed on vagal afferent terminals innervating the GI tract.

VAN-Specific GHSR Knockdown Alters Meal Patterns, but Not Cumulative Food Intake or Entrained Feeding

Spontaneous meal-pattern analyses were conducted to examine the effect of VAN-specific GHSR knockdown on feeding behavior. Results over 7 days revealed a significant increase in meal frequency in the VAN-specific GHSR knockdown group compared with controls

(Figures 3A and 3B; $p < 0.05$), coupled with a nonsignificant trend in reduced average meal size (Figures 3C and 3D;$p = 0.09$) such that no significant differences were observed in cumulative 24 h chow intake (Figures 3E and 3F). VAN-specific GHSR knockdown had no significant effect on any feeding parameters when analyses were restricted to the light cycle (data not shown).

In the meal entrainment procedure (Figure 3G), food access is restricted to a 4 h period per day over 8 days. Results showed no differences between VAN-specific GHSR knockdown and controls in total food consumed by day over the 8-day period (Figure 3H; $p < 0.05$). These findings suggest that VAN-specific GHSR knockdown does not affect the learning required to adapt to meal entrainment scheduling. Furthermore, food intake data from day 1 reveal that there were no group differences following either 1 h (control = 5.62 g [SEM ± 0.51], VAN GHSR KD = 5.45 g [SEM ± 0.37]) or 4 h (Figure 3G) of refeeding after an unanticipated fast.

VAN-Specific GHSR Knockdown Slows Gastric Emptying Rate

Using a gavage-based acetaminophen approach [10], we investigated the effect of VAN-specific GHSR knockdown on gastric emptying rate. Results revealed a significant interaction between treatment and time, as well as a significant main effect of time (Figure 3I; $p < 0.05$). Post hoc analysis revealed a significant group effect at the 90 min time point, indicating that VAN-specific GHSR knockdown slows gastric emptying rate.

VAN-Specific GHSR Knockdown Increases Body Weight and Lean Mass

VAN-specific GHSR knockdown increased body weight versus controls (Figure 3J; $p < 0.05$). NMR body composition imaging at 23 weeks post-surgery revealed that this effect was based on increased lean mass in the knockdown animals compared with controls (Figure 3L; $p < 0.05$) with no differences in fat mass or the ratio of fat-to-lean mass (Figures 3M and 3N).

VAN-Specific GHSR Knockdown Impairs Glucose Tolerance and Increases Postprandial Insulin Levels

We tested the effect of VAN-specific GHSR knockdown in an i.p. glucose tolerance test. Results revealed a significant interaction between treatment and time and a significant main effect of time. Post hoc analysis revealed a significant group effect at the 30-min time point (Figure 3O; $p < 0.05$), when knockdown animals had elevated blood glucose levels. Area under the curve analysis further confirmed that knockdown animals had impaired glucose tolerance (Figure 3P; $p < 0.05$). To investigate potential underlying mechanisms, we tested the effect of VAN-specific GHSR knockdown on postprandial serum insulin levels. Results revealed a significant main effect of group, where knockdown animals had increased insulin levels versus controls (Figure 3Q; $p < 0.05$). These results suggest that the impairment in glucose tolerance in knockdown animals is mediated by insulin intolerance and not by reduced insulin production and/or secretion.

VAN-Specific GHSR Knockdown Impairs HPC-Dependent Memory and Reduces HPC BDNF Levels

Novel object in context (NOIC) is a test of HPC-dependent contextual episodic memory (Figure 4A). Results reveal that VAN-specific GHSR knockdown animals had a significantly reduced shift from baseline of novel object investigation relative to control animals (Figure 4B; $p < 0.05$). There was no difference between groups in the exploration of the non-novel object on test day (control, 18.51 ± 0.96 s; knockdown, 21.38 ± 1.77 s). These findings indicate that VAN GHSR signaling is required for HPC-dependent contextual episodic memory in rats.

To confirm that decreased novel object exploration in knockdown animals was not secondary to a general avoidance of novel objects due to altered anxiety, we tested anxiety-like behavior using the zero maze test (Figure 4C). Results show no differences between groups in anxiety-like behavior for either time in open zones (Figure 4D) or open zone entries (Figure 4E).

The HPC-dependent memory impairments seen in the NOIC test may be based, in part, on reduced neurotrophic signaling in the dorsal CA3 subregion. Immunoblot analyses revealed decreased protein levels of brain-derived neurotrophic factor (BDNF) in CA3-enriched brain tissue punches of VAN-specific GHSR knockdown animals compared with controls (Figures 4F and 4G; $p < 0.05$). No group differences were identified in dCA1+dDG-enriched brain punches for expression of either BDNF (Figure 4H) or the proliferation marker, doublecortin (Figure 4I).

VAN-Specific GHSR Knockdown Does Not Affect Appetitive Contextual or Spatial Memory

We investigated the effect of VAN-specific GHSR knockdown on a spatial foraging task (Figure S1A), which tests the ability for animals to learn and remember the spatial location of food. Results revealed no group differences in latency to correct hole (Figure S1B), nor errors before correct hole entry during training (Figure S1C). There were also no group differences in the memory retention probe, as measured by the correct+adjacent holes investigated/total holes investigated (Figure S1D). In a test of conditioned place preference expression for a high-fat diet (Figure S1E), there were no group differences in preference for the food-paired context (expressed as shift from baseline) (Figure S1E).

DISCUSSION

Paracrine signaling by gut hormones via the vagus nerve is a critical pathway through which the GI tract communicates to the brain to regulate energy balance and metabolic function [11–14]. However, little is understood about the neurobiological mechanisms of VAN paracrine signaling. The present results reveal that the stomach-derived orexigenic hormone ghrelin acts via VAN GHSR signaling to influence various aspects of feeding behavior and metabolic processes. VAN-specific GHSR knockdown increased meal frequency with a trend toward decreased meal size compared with controls such that there were no differences in cumulative intake between groups. Additionally, metabolic parameters were disrupted by VAN GHSR knockdown, including impaired glucose tolerance driven by insulin resistance,

slower gastric emptying rate, and increased body weight driven by increased lean mass. These findings indicate that VAN ghrelin/GHSR signaling plays an endogenous role in normal feeding behavior and metabolism.

VAN-specific GHSR knockdown impaired hippocampal-dependent contextual episodic memory, an outcome that may be driven in part by reduced BDNF expression in the dorsal CA3 subregion. These findings identify a paracrine mechanism for our previous findings demonstrating that gut-specific VAN ablation impairs hippocampal-dependent memory and reduces HPC BDNF [3]. It is possible that the observed memory impairments in the present study are functionally related to the increased spontaneous meal frequency following VAN-specific GHSR knockdown. For example, reversible inhibition of hippocampal neurons reduces the intermeal interval in rodents [15–18]. Similarly, interfering with meal-related episodic memory in humans increases subjects' self-reported hunger rating [19]. However, it is also possible that the increased meal frequency effects are based, in part, on the reduced gastric emptying rate in GHSR VAN knockdown rats, which may contribute to reduced meal size with a compensatory increase in meal frequency. However, this possibility is less likely as the trend for reduced spontaneous meal size failed to reach statistical significance. These results collectively identify VAN GHSR signaling as a potential physiological link between episodic memory and feeding behavior.

In addition to the vagal paracrine pathway investigated in the present study, ghrelin influences food intake, metabolism, and memory function via a putative blood-to-brain pathway [20–23]. However, the present study supports a role for VAN ghrelin/GHSR signaling that is functionally distinct from brain GHSR signaling with regard to meal patterns and entrained feeding. For example, activation of GHSR signaling in the ventral hippocampus increases dark cycle food intake via increased meal size without influencing meal frequency [24], whereas VAN-specific GHSR knockdown in the present study increased meal frequency without affecting cumulative intake. In addition, VAN-specific GHSR knockdown does not influence food intake in a meal entrainment schedule that has been shown to increase peripheral ghrelin release immediately prior to meal access [25], whereas food consumption in meal-entrained rats is reduced by ventral hippocampus GHSR blockade [26]. These findings highlight examples in which ghrelin differentially influences behavior via VAN versus brain signaling pathways.

Electrophysiological results from the present study reveal that ghrelin functionally excites VAN neural responses in a GHSR-dependent manner. Given that ghrelin circulation in this experiment was gut-restricted and thus precluded from access to somatic GHSRs within the NG, these results are likely based on GHSRs expressed on vagal afferent terminals innervating the GI tract. Notably, VAN GHSR knockdown reduced the VAN neural response to ghrelin, but not CCK, thus further confirming the specificity of the GHSR-targeted RNAi approach. Complementing present findings that ghrelin engages VAN signaling both electrophysiologically and functionally, additional results show that SDV attenuates the hyperphagic effects of peripheral ghrelin during the nocturnal phase. These findings are consistent with a previous report by Date et al. that evaluated ghrelin-stimulated hyperphagia in SDV rats, albeit before the complete recovery from SDV surgery [7]. In contrast, Arnold et al. reported that SDV has no effect on ghrelin-mediated hyperphagia in rats after an

extensive recovery period [27]. The discrepancies between this latter report and the present results may be based on methodological differences between experiments, as our feeding analyses were conducted in the dark cycle, whereas Arnold and colleagues examined intake during the light cycle. A potential effect of photoperiod may be, in part, due to the diurnal rhythm of NG *Ghsr* mRNA expression, with expression higher during the light versus the dark cycle [9]. Differences in results between studies may also be based on circadian variation in gastric VAN mechanosensitivity, which is increased during the light versus the dark cycle [28]. Future research will be required to determine the importance of photoperiod on the role of the vagus nerve in mediating the orexigenic effect of ghrelin.

The present results collectively reveal a novel role for endogenous VAN GHSR signaling in feeding behavior, metabolism, and HPC-dependent memory. These findings not only identify a novel neurobiological mechanism for ghrelin's effects on various physiological and behavioral processes, but are also consistent with emerging evidence that gut peptides engage in functionally relevant paracrine signaling via the vagus nerve.

STAR★METHODS

RESOURCE AVAILABILITY

Lead Contact—Further information and requests for resources and reagents should be directed to and will be fulfilled by the Lead Contact, Dr. Scott Kanoski (kanoski@usc.edu).

Materials Availability—The GHSR RNAi virus used in this study is available through Vector Biolabs (https://www.vectorbiolabs.com/).

Data and Code Availability—The datasets generated during this study are available in the Open Science Framework Repository [https://osf.io/rufcz/].

EXPERIMENTAL MODEL AND SUBJECT DETAILS

For electrophysiological experiments, male Wistar rats (Charles River; 3–6 weeks old, 50–120 g) were housed in specific-pathogen free cages on a 12 h:12 h light/dark cycle and had access to standard rat chow *ad libitum*. All procedures were approved by the University of Florida Institute of Animal Care and Use Committee.

For the gastric emptying experiment, adult male Sprague-Dawley rats (Charles River; 250–265 g on arrival) were individually housed with *ad libitum* access (except where noted) to water and rodent chow (Purina 5001) on 12 h/2 h light/dark cycle. All procedures were approved by the University of Pennsylvania Institutional Animal Care and Use Committee.

For evaluation of Ghsr expression in the nodose ganglia of mice, adult male C57BL/6J mice (originally obtained from Jackson, bred in-house) were group housed with *ad libitum* access to rodent diet (PicoLab Rodent Diet 20, #5053) on a 13:11 h light/dark cycle. All procedures were approved by the Children's Hospital of Los Angeles Institute of Animal Care and Use Committee.

For all other experiments, Adult male Sprague–Dawley rats (Envigo; 250–275 g on arrival) were individually housed with *ad libitum* access (except where noted) to water and chow (LabDiet 5001, LabDiet, St. Louis, MO) on 12 h:12 h light/dark cycle. All procedures were approved by the University of Southern California Institute of Animal Care and Use Committee. For all experiments, procedures conformed to the relevant regulatory guidelines.

METHOD DETAILS

Vagotomy—Rats were habituated to liquid diet (Research Diets; AIN76A) for one day prior to surgery. Following a 24 h fast and under ketamine (90 mg/kg), xylazine (2.7 mg/kg), and acepromazine (0.64 mg/kg) anesthesia and analgesia (a subcutaneous injection of carprofen [5 mg/kg]), complete subdiaphragmatic vagotomy (SDV) was performed (n = 6) as described previously [29]. Animals were randomized such that body weight between groups was not significantly different at time of surgery (Sham: 310.9 g ± 3.2; SDV: 314.2 g ± 3.6). Briefly, a midline abdominal incision was made, the stomach was retracted caudally, and the liver was retracted cranially to expose the esophagus. The dorsal and ventral trunks of the vagus were then dissected from the esophagus. Each vagal trunk was ligated twice with a surgical thread at an interval of 1–2 cm, and then cauterized between the ligatures. In sham surgeries (n = 7), the trunks were exposed but the vagus nerve was not ligated or cauterized. The incision was then closed with running sutures along the abdominal wall and stop sutures along the skin. Rats were allowed to recover on liquid diet for 3 days, and then were maintained on a powered chow diet for the remaining recovery period up to two weeks post-surgery, then were returned to a standard chow diet. Behavioral testing was performed approximately 3 months after surgery. After behavioral testing, SDV was verified functionally with intraperitoneal cholecystokinin (CCK)-induced food intake reduction as described [30, 31]. Briefly, the functional verification consists of analysis of food intake following intraperitoneal (IP) cholecystokinin (CCK-8, 2 mg/kg; Cat# 4033010, Bachem, Torrance, CA) or saline injections (treatments given counterbalanced on separate days) after an overnight fast. SDV rats were included in the statistical analysis if CCK treatment resulted in a less than 30% reduction of their food intake, as described [32]. No animals were removed for analyses based on these criteria.

Food analyses following intraperitoneal ghrelin administration—The effect of vagotomy on IP ghrelin-mediated hyperphagia was measured in rats maintained on *ad libitum* chow and water. Food was removed 1 h prior to injections. IP ghrelin (0, 20, or 40 mg/kg body weight, Bachem, Cat. #4033076) or saline (control) was administered immediately prior to dark onset. Food was returned at dark onset and cumulative 2 h chow intake was recorded. Each animal received all three treatments (within-subjects design, randomized in a counterbalanced order, vagotomy n = 6, sham n = 7) with each treatment day separated by 2 days.

RNA interference-mediated VAN-specific GHSR knockdown—For RNA interference (RNAi)-mediated in vivo knockdown of Ghsr gene expression, short hairpin RNA (shRNA) targeting Ghsr mRNA was cloned and packaged into an adeno-associated virus (AAV2; Vector Biolabs, Malvern, PA) and co-expressing green fluorescent protein (GFP), with both casettes downstream of the U6 promoter (titer 1⁄4 1.7e13 GC/mL; AAV2-

GFP-U6-rGHSR-shRNA). The sequence of the shRNA is as follows: CCGGACTGCAACCTGGTGTCCTTTGCTCGAGCAAGGACACCAGGTTGCAGTTTTTG. A scrambled shRNA, GFP-expressing AAV2 downstream of a U6 promoter (titer 1⁄4 1.7e13 GC/mL; AAV2-GFP-U6-Scrmb-shRNA) was used as a control (Cat # 7041, Vector Biolabs, Malvern, PA).

Nodose ganglion injections were performed as previously described [3, 13]. Briefly, the day before surgery for nodose ganglia AAV injections, chow was removed and rats were given 130mL of diluted condensed milk. Animals were randomized into groups such that body weight between groups was not significantly different at time of surgery. The day of surgery, rats were anesthetized via intra-muscular injections of ketamine (90 mg/kg), xylazine (2.8 mg/kg), and acepromazine (0.72 mg/kg) and were given a preoperative dose of analgesic (a subcutaneous injection of carprofen [5 mg/kg]). Once the appropriate plane of anesthesia was reached, a midline incision was made along the length of the neck. The vagus nerve was separated from the carotid artery with Graefe forceps until the nodose ganglion was visible and accessible. A glass capillary (20 μm-50 μm tip, beveled 30° angle) attached to a micromanipulator was used to position and puncture the nodose ganglion and 1.5 μL volume of AAV2-GFP-U6-rGHSR-shRNA (or the control AAV) was injected with a Picospritzer III injector (Parker Hannifin; Cleveland, OH) within the nodose ganglion at two sites: 0.75 μL of virus was delivered rostral to the laryngeal nerve branch, and the remaining 0.75 μL of virus was delivered caudal to the laryngeal nerve branch. The same procedure was performed for both nodose ganglia before the skin was closed with interrupted sutures. Postoperatively, rats were recovered to sternal recumbency on a heat pad and then returned to their home cage. Analgesic (5 mg/mL carprofen subcutaneously) was given once per day for 3 days after surgery. Condensed milk was given on day 1 and day 2 postoperatively (130 mL/day), with chow reintroduced on day 3 alongside the 130 mL condensed milk. On day 4 and onward, rats were returned to *ad libitum* access to chow. All subsequent analyses occurred after three weeks of post-surgical viral transfection. While our AAV was applied directly to the nodose ganglia, the subsequent RNAi process would interfere with all cytoplasmic gene expression, including for the production GHSR protein that is trafficked to the vagal terminals. The DAPR electrophysiological approach (see next section) was used to further investigate the functional VAN response to ghrelin at the level of the terminals after GHSR knockdown.

Modified decorticated artificially perfused rat (DAPR) preparation for gut-restricted ghrelin infusion and afferent vagal nerve recordings *in situ*—Wistar rats (male, 4 weeks old, 50–60 g, N = 8) received unilateral injection of AAV2-GFP-U6-rGHSR-shRNA in either the left (LNG) or right (RNG) nodose ganglia (n = 4 per group) and a control virus (AAV-hSyn-hChR2(h134R)-eYFP, Addgene, Cat# 26973-AAV1) on the contralateral side. Three weeks after viral injections in nodose ganglia, we performed direct electrophysiological recordings of afferent vagal activity rostral to both LNG and RNG simultaneously using a modified decorticated artificially perfused rat (DAPR) *in situ* preparation 2 weeks following viral injections in nodose ganglia. The modification to the previously described DAPR [33–35] included retention of an intact GI tract with a separate perfusion system allowing specific targeting of GI vagal afferents by delivering ghrelin or

CCK via arterial GI circulation (see schematics of the modified *in situ* DAPR in Figure 2A). Wistar rats (male, 6 weeks old, 100–120 g, n = 8) were briefly anesthetized with isoflurane (4%), exsanguinated, decorticated (decerebrated at the precollicular level as originally described in [36]), and immediately submerged into ice-chilled artificial cerebrospinal fluid (aCSF; composition in mM: 125 NaCl, 24 NaHCO3, 3KCl, 2.5 CaCl2, 1.25 MgSO4 and 1.25 KH2PO4, 10 dextrose, pH 7.3) (Sigma-Aldrich and Fisher, USA). The skin was removed and the chest cavity was cut open keeping the diaphragm intact. Inferior vena cava and descending aorta were clamped immediately rostral to the diaphragm to isolate the brainstem from GI circulation (Figure 2A). The descending aorta was cannulated immediately above the clamp with a double lumen catheter (Braintree Scientific) for rostral perfusion of the brainstem as previously described [35]. Below the diaphragm, descending aorta was cannulated with a separate double lumen catheter (Braintree Scientific) immediately above the iliac bifurcation for perfusion of the GI tract (Figure 2A). The adjacent abdominal vein was severed in the most caudal lumbar region in order to allow release of the GI perfusate and its collection into a separate chamber for recirculation throughout the experiment. Both the right and left nerves were transected rostral to the ganglia to ensure recordings were of exclusively afferent vagal activity in both cervical vagal trunks simultaneously, without interference of the parasympathetic efferent signals that also travel via the vagus nerve. Following the surgery, the preparation was transferred to an acrylic perfusion chamber, and brainstem and GI were immediately perfused via the two implanted cannulae using separate warmed Ringer's solutions (32–33°C) containing Ficoll PM70 (1.25%, Sigma-Aldrich, USA) bubbled with 95% O_2/5% CO_2 and pumped through in-line bubble traps and a filter (polypropylene mesh; pore size: 40 mm, Millipore) via two peristaltic pumps. Neuromuscular paralysis in the region above diaphragm was produced by addition of vecuronium bromide (2–4 mg/mL, Bedford Laboratories, USA) directly to the brainstem perfusate to eliminate the movement noise on nerve recordings. Perfusion pressures were measured via one lumen of the double-lumen catheters using two pressure transducers connected to an amplifier. Simultaneous recordings of the left and right afferent nerve activity (LNG and RNG; Figure 2A) were obtained using glass suction electrodes (tip diameter, 0.2–0.3 mm), amplified (20–50K) and filtered (3–30K), sampled at 5 kHz (CED, Cambridge) and monitored using Spike2 (CED). The perfusate flows (19–24 mL/min for brainstem and 1.5–3.5 mL/min for GI perfusion) were adjusted to mimic physiologic perfusion levels and maintain the health of the preparation [33–35, 37]. Vasopressin (1.25–4 nM final concentration, Sigma-Aldrich, USA) was added to the brainstem perfusate to increase vascular resistance and aid in maintenance of adequate brainstem perfusion to preserve autonomic reflexes [33–35]. Bilateral vagal afferent responses were simultaneously recorded in response to slow bolus intra-arterial GI infusion of 1) saline (0.9%, 100 ml), 2) ghrelin (Phoenix Peptide, 031–31, 5nmol in 100 ml saline), and 3) CCK (Bachem, Cat# 4033010, 1 μg in 100 μL saline) within each preparation, always in this order. To account for the 400 μL dead space in the tubing, 400 mL saline was additionally administered after each infusion. CCK was delivered 5 min following the ghrelin injection to assess specificity of shRNA mediated knockdown.

For data analysis and comparison, the maximum amplitude of immediate afferent vagal nerve activation of integrated ∫LNG and ∫RNG (time constant = 50 ms) to ghrelin or CCK

administration in the GI tract was calculated as change (Δ) in μV from baseline representing the period of nerve activity recorded immediately following control saline injection. Comparisons were made either 1) between shRNA and control injected nodose ganglia within every animal, or 2) between left and right control injected nodose ganglia between subjects, and averaged for all preparations. Immediately following recordings, nodose ganglia were harvested for quantification of knockdown via gene expression (following three weeks of post-surgical viral transfection) (control n = 12 ganglia, knockdown n = 8 ganglia, left/right counterbalanced).

Meal pattern—Meal size, meal frequency, and cumulative 24 h food intake was measured using the Biodaq automated food intake monitors (Research Diets, New Brunswick, NJ). Animals (control n = 13, knockdown n = 12) were acclimated to the Biodaq on *ad libitum* chow for 3 days. Data were collected over a 7-day period (meal parameters: minimum meal size = 0.2g, maximum intermeal interval = 600 s).

Meal entrainment—Animals were subjected to a meal-entrainment schedule as previously described [26]. Briefly, animals (knockdown n = 13, control n = 11) were limited to chow access for 4 h daily (for the first 4 h of the dark cycle) over an 8-day period. Cumulative 4 h food intake was recorded daily and water was available *ad libitum*.

Gastric emptying—A gavage-based acetaminophen approach was used to measure gastric emptying rate, as this approach is standard in field for both humans and rats [10, 38, 39]. Animals (knockdown n = 6, control n = 6) were habituated to gavage prior to testing. Food was removed 16 h before testing (last 4 h of dark cycle plus full 12 h light cycle) to limit the influence of variability in stomach contents on gastric emptying rate. At dark onset, rats were gavaged with 6 mL of a test meal of vanilla-flavored Ensure (Abbott Laboratories, Chicago, IL; 1.42 kcal/mL) containing 40 mg acetaminophen (Sigma-Aldrich, Cat #PHR1005). Tail vein blood (~200μl) was collected immediately prior to dark onset/gavage (0; baseline) and 30, 60, and 90 min after dark onset/gavage with pre-coated EDTA microvette (Sarstedt, Nümbrecht Germany, supplier Fisher Scientific Cat# NC9976871). Tubes were immediately placed on wet ice, centrifuged, and plasma was collected and stored at −80°C until further processing. Acetaminophen concentrations were measured with a commercial kit (Cambridge Life Sciences, Ely, England K8003) adapted for a multi-well plate reader (Tecan Sunrise, Männedorf, Switzerland) according to manufacturer's instructions. Each sample was run in duplicate.

Body weight and body composition—Throughout all knockdown experiments, animals (knockdown n = 13, control n = 11) were weighed daily just prior to dark cycle onset to examine the effect of VAN-specific GHSR knockdown on body weight. At the conclusion of behavioral experiments, the Bruker LF90II nuclear magnetic resonance (NMR) minispec was used for non-invasive measurement of fat mass and lean mass to determine the effect of VAN-specific GHSR knockdown on body composition.

Glucose tolerance test—Animals (knockdown n = 12, control n = 11) were food restricted 20 h prior to an intraperitoneal glucose tolerance test (IP-GTT). Immediately prior to the test, baseline blood glucose readings were obtained from the tail tip and recorded by a

blood glucose meter (One Touch Ultra2, LifeScan, Milpitas, CA). Each animal was then injected intraperitoneally (IP) with dextrose solution (1g dextrose / kg BW). Blood glucose readings were obtained at 30, 60, 90, and 120 min after IP injections.

Postprandial serum insulin—Animals (knockdown n = 8, control n = 6) were food restricted 24 h prior to a postprandial serum insulin test. Immediately prior to the test (at dark onset), baseline blood collections were taken from the tip of the tail (time point 0). Each animal was then allowed to consume the entirety of a 3g meal of powdered rodent chow, to which they had previously been habituated. All animals finished the meal between 15 and 20 min post meal access. Blood samples were then obtained from the tip of the tail at 10, 25, and 40 min after meal termination. Blood samples were allowed to clot at room temperature, centrifuged, serum was collected and stored at −80°C until further processing. Serum insulin concentrations were measured with a commercial kit (Crystal Chem, Elk Grove Village, IL; Cat #90010) adapted for a multi-well plate reader (BioRad iMark Microplate Reader, BioRad Hercules, CA) according to manufacturer's instructions. Each sample was run in duplicate.

Novel object in context—To test the effect of VAN-specific GHSR knockdown on HPC-dependent contextual episodic memory, animals (knockdown n = 10, control n = 11) were tested in the Novel Object in Context (NOIC) procedure. Briefly, rats are habituated to Context 1, a semi-transparent box (15 in W × 24 in L × 12 in H) with orange stripes and Context 2, a gray opaque box (17 in W × 17 in L × 16 in H). Contexts and objects are cleaned with 10% ETOH between each animal. On Day 1following habituation (D1) at dark onset prior to the first meal, each animal is exposed to two distinct objects: a Coca Cola can (Object A) and a stemless wine glass (Object B) for 5 min in Context 1. On Day 2, the animals are exposed to duplicates of either Object A or Object B (counterbalanced by experimental group) for 5 min in Context 2. On Day 3 (D3), the animals are placed in the previous day's location (Context 2) with Object A and Object B during a 5 min test period. Investigation time ($T_{\hat{n}}$) of both objects is measured by AnyMaze Behavior Tracking Software (Stoelting, Wood Dale, IL). Investigation is defined as sniffing or touching the object with the nose or forepaws. The task is scored by calculating the novel object investigation shift from baseline (from D1). If Object A is the novel object, shift from baseline is calculated as:

$$\frac{T_1\ of\ obj.\ A\ on\ D3}{T_1\ of\ obj.\ A\ on\ D3 + T_1\ of\ obj.\ B\ on\ \mathrm{D3}} - \frac{T_1\ of\ obj.\ A\ on\ D1}{T_1\ of\ obj.\ A\ on\ D1 + T_1\ of\ obj.\ B\ on\ D1} = \underset{from\ baseline}{Novel\ object\ shift}$$

Normal rats will preferentially investigate the object that had not been previously seen in Context 2, given that it is a familiar object that is now presented in a novel context. This will result in a novel object shift from baseline that is increased compared with zero.

Zero maze—To examine the effect of VAN-specific GHSR knockdown on anxiety-like behavior, animals (knockdown n = 13, control n = 11) were tested in the zero maze task. The zero maze apparatus is an elevated circular track, divided into four equal length sections. Two zones are open with 3 cm high curbs ('open zones'), whereas the two other zones are

closed with 17.5 cm high walls (‘closed zones’). Animals were placed in the maze for a single, 5 min trial, in which animal location was measured by AnyMaze Behavior Tracking Software (Stoelting, Wood Dale, IL). The apparatus was cleaned with 10% ethanol in between animals. The dependent variables were the number of open section entries and total time spent in open sections (defined as the head and front two paws in open sections), which are each indicators of anxiolytic-like behavior in this procedure. A diagram of the zero maze paradigm is included in Figure 4C.

Tissue collection—Rats and mice were fasted for 12 h before all tissue extractions. Rat brains were rapidly removed from the skull and flash frozen in 30°C isopentane on dry ice, then stored at −80°C to until further processing. Nodose ganglia to be processed for gene expression were flash frozen on dry ice and stored at −80°C to await further processing (see qPCR). Nodose ganglia to be processed for histology were postfixed in ice-cold 4% paraformaldehyde for 2 h, transferred to 25% sucrose at 4C, and remained in sucrose for at least 24 h before sectioning (see Histology or FISH). Nodose ganglia for qPCR analyses were flash frozen in −30°C isopentane on dry ice, then stored at −80°C to await further processing.

Immunoblotting—Tissue punches of brain regions of interest (2.0mm circumference, 1–2mm depth) were collected from brains (knockdown n = 13, control n = 9) using a Leica CM 1860 cryostat (Wetzlar, Germany) and anatomical landmarks were based on the Swanson rat brain atlas [40]. Tissue punches were enriched with the dorsal cornu ammonis area 1 and dorsal dentate gyrus (dCA1+dDG; Swanson atlas levels 29–30), and the cornu ammonis area 3 (dCA3; atlas levels 29–30). Proteins in brain lysates were separated using sodium dodecyl sulfate polyacrylamide gel electrophoresis, transferred onto poly-vinylidene difluouride membranes, and subjected to immunodetection analysis using enhanced chemiluminescence (Chemidoc XRS, BioRad). A rabbit anti-brain-derived neurotrophic factor antibody (1:500, Santa Cruz Biotechnology, Catalog # sc-20981) was used to evaluate the concentration of brain-derived neurotrophic factor (BDNF) relative to a loading control signal detected by a rabbit anti-β-actin antibody (1:5000, Santa Cruz Biotechnology, Catalog # NB600–503). A rabbit anti-doublecortin antibody (1:500, Abcam, Catalog # ab18723) was used to evaluate the concentration of doublecortin (DCX) relative to a loading control signal detected by a rabbit anti-β-tubulin antibody (1:5000, Cell Signaling, Catalog #2128S). Blots were quantified with densitometry analysis using ImageJ as previously described [3].

Fluorescent *In Situ* Hybridization (FISH)—Nodose ganglia (n = 3 animals, both right and left ganglia for a total of 6 ganglia) were cut on the Leica CM 1860 cryostat (Wetzlar, Germany) at 20 μm and mounted directly onto slides. Slides were washed 5x in KPBS for 5 min each. Sections were then pretreated by incubating them at 37°C in incubation buffer (100mM Tris buffer and 50mM EDTA in distilled deionized water, pH 8) with 0.001% Proteinase K (Sigma P2308) for 30 min, followed by a 3 min wash in incubation buffer alone and a 3 min rinse in 100mM Triethanolamine in water (pH 8). Sections were then incubated with 0.25% acetic anhydride in 100 mM triethanolamine for 10 min at room temperature followed by 2 × 2 min washes in saline-sodium citrate buffer (1% citric acid trisodium/2% sodium chloride in water (pH 7.0)). Slides were dehydrated in increasing

concentrations of ethanol solution (50%, 70%, 95%, 100%, 100%) for 3 min each and air-dried prior to hybridization. For hybridization, a hydrophobic barrier was drawn around each section and 3 to 4 drops of the probes (*Ghsr1a* mRNA probe (#431991), *NeuN* mRNA probe (#436351-C2), and Dapi mRNA probe (#323108), all Advanced Cell Diagnostics; Newark, CA) were placed on each tissue section. Slides were incubated with the probes at 40°C for 3 h in a HybEz oven (Advanced Cell Diagnostics). Following a 2 min wash with wash buffer (RNAscope, Advanced Cell Diagnostics 320058) reagents from RNAscope Fluorescent Multiplex Detection Reagent Kit (Advanced Cell Diagnostics, 320851) were applied in order to amplify the probe signals, with AMP1 applied for 45 min, AMP2 for 30 min, AMP3 for 45 min, and AMP4 for 30 min. Incubation steps occurred at 40°C, and a 2 min wash followed each amplification step. Slides were coverslipped with ProLong Gold Antifade mounting medium (Cell Signaling, 9071S). Photomicrographs were acquired using a Nikon 80i (Nikon DS-QI1, 1280 × 1024 resolution, 1.45 megapixel) under epifluorescent illumination. The percentage of *NeuN*+ nodose ganglia neurons that co-express Ghsr was quantified by a researcher blinded to experimental treatment using Nikon Elements software.

Quantitative polymerase chain reaction (qPCR)—To quantify knockdown of Ghsr mRNA expression, quantitative polymerase chain reaction (qPCR) was performed on nodose ganglia, as previously described [41, 42], with left (LNG) and right nodose ganglia (RNG) analyzed separately. Briefly, total RNA for rat nodose ganglia was extracted according to manufacturer's instructions using the RNeasy Lipid Tissue Mini Kit (Cat # 74804, QIAGEN; Hilden, Germany) for both the shRNA experiments (knockdown n = 8 ganglia, control n = 12 ganglia, left/right counterbalanced) and the laterality experiments in the rat (n = 10 ganglia; left n = 5 ganglia, right n = 5 ganglia). For the laterality experiments in the mice, total RNA for mouse nodose ganglia (n = 8 ganglia; left n = 4 ganglia, right n = 4 ganglia) was extracted according to manufacturer's instructions using the RNeasy Micro Kit (Cat # 74004, QIAGEN). RNA was reverse transcribed to cDNA using the Quantitect Reverse Transcription Kit (QIAGEN), and amplified using the TaqMan PreAmp Master Mix (Cat #4391128, ThermoFisher Scientific, Waltham, MA). qPCR was performed with TaqMan Fast Advanced Master Mix (Cat#4444557, Applied Biosystems, Foster City, CA) using the Applied Biosystems QuantStudio 5 Real-Time PCR System (ThermoFisher Scientific). Negative reverse-transcribed samples were generated and all reactions were carried out in triplicate, and control wells without cDNA template were included. The following probes (TaqMan, Applied Biosystems) were used: Rat *Ghsr* [growth hormone secretagogue receptor]: Rn00821417_m1, Rat *Mchr1* [melanin concentrating hormone receptor 1]: Rn00755896_m1, Rat *Cnr1* [cannabinoid receptor 1]: Rn00562880_m1, Rat *Gapdh* [Glyceraldehyde 3-phosphate dehydrogenase]: Rn01775763_g1, Mouse *Ghsr*: Mm00616415_m1, Mouse *Gapdh*: Mm99999915_g1. To determine relative expression values, the $2^{-\Delta\Delta CT}$ method was used [9], where triplicate Ct values for each sample were averaged and subtracted from those derived from *Gapdh*.

Spatial foraging task—To test the effect of VAN-specific GHSR knockdown on a food seeking task requiring visuospatial learning and memory, we tested the animals on a novel spatial foraging task modified from the traditional Barnes maze procedure [43]. Briefly, rats are trained on a Barnes maze apparatus (elevated circular maze with 18 holes around the

perimeter) with fixed spatial cues on the walls. Rats undergo training (four consecutive training days, two trials per day, trials 120 min apart) to learn the fixed location of a hidden escape tunnel that contains five highly palatable sucrose pellets located in one of the 18 holes around the maze. Rats are tested in a single 2 min probe trial in which the hidden tunnel and sucrose pellets are removed. During the probe trial, normal rats will preferentially investigate the hole in which the sucrose pellets and hidden tunnel were previously located.

Conditioned place preference—To test the effect of VAN-specific GHSR knockdown on contextual learning for a food reward, rats underwent a conditioned place preference (CPP) behavioral paradigm. Procedures followed the CPP protocol as previously described [44]. Briefly, rats were habituated to the CPP apparatus, which consists of two conjoined plexiglass compartments with a guillotine door in the center (Med Associates, St. Albans, VT). The two compartments (contexts) differ in wall color and floor texture. Habituation occurred with the CPP apparatus door open, allowing them to freely explore each context. Time in each context was measured using AnyMaze Behavior Tracking Software (Stoelting, Wood Dale, IL). For each rat, the context that was least preferred during habituation was designated as the food-paired context for subsequent training. CPP training consisted of one 20 min session per day over 16 consecutive days, with eight food-paired and eight non-food paired counterbalanced sessions occurring in total. The CPP apparatus door was closed during all training sessions, restricting rats to one context only. During food-paired training sessions, rats were isolated in the food-paired context with 5 g of palatable food (45% kcal high fat/sucrose diet [D12451, Research Diets, New Brunswick, NJ]) placed on the chamber floor. During non-food paired training sessions, rats were isolated in the non-food-paired context with no food present. The CPP test occurred two days after the last training session using a between-subjects design. During testing, the CPP apparatus door was opened, and the rats were allowed to freely explore both contexts during a 15 min trial. For all habituation, training and testing, the apparatus was cleaned with 10% ethanol in between animals. Time in each context was measured using AnyMaze Behavior Tracking Software (Stoelting, Wood Dale, IL). The dependent variable was the percentage shift in preference for the food-associated context during testing compared with the baseline session.

QUANTIFICATION AND STATISTICAL ANALYSIS

Data are presented as mean ± SEM. Sample size n for each experiment (representing number of animals) are included in the STAR methods. Statistical tests were performed using Graphpad (San Diego, CA): For comparisons of over time of body weight, food intake (cumulative 24 h intake, meal pattern, meal entrainment), gastric emptying, blood glucose, and postprandial insulin, groups were compared using a two-way repeated-measures ANOVA (group × time) and significant ANOVAs were analyzed with a Fisher's LSD posthoc test where appropriate. For comparisons of food intake after IP ghrelin treatment, groups were compared using a two-way repeated-measures ANOVA (surgery × treatment). Paired two-sample two-tailed Student's t tests were used for comparison of within-animal neural responses in the DAPR experiments. Unpaired, two-sample, two-tailed Student's t tests were used for all other analyses. Differences were considered statistically significant when $p < 0.05$. Outliers were identified as being more extreme than the Median ± 1.5 *

Interquartile Range. Assumptions of normality (Shapiro-Wilk), homogeneity of variance (Spearman's), and independence were met when required.

Supplementary Material

Refer to Web version on PubMed Central for supplementary material.

ACKNOWLEDGMENTS

This study was supported by NIH grants DK104897 (S.E.K.), DK118402 (S.E.K.), DK116558 (A.N.S.), DK118944 (C.M.L.), DK120162 (H.S.W.), DK021397 (H.J.G.), AT010192 (J.Z.), DK094871 (G.d.L.), and DK116004 (G.d.L.), and the University of Sydney Special Studies Program (J.W.P.).

REFERENCES

1. Powley TL, and Phillips RJ (2004). Gastric satiation is volumetric, intestinal satiation is nutritive. Physiol. Behav 82, 69–74. [PubMed: 15234593]
2. Klarer M, Weber-Stadlbauer U, Arnold M, Langhans W, and Meyer U (2019). Abdominal vagal deafferentation alters affective behaviors in rats. J. Affect. Disord 252, 404–412. [PubMed: 31003109]
3. Suarez AN, Hsu TM, Liu CM, Noble EE, Cortella AM, Nakamoto EM, Hahn JD, de Lartigue G, and Kanoski SE (2018). Gut vagal sensory signaling regulates hippocampus function through multi-order pathways. Nat. Commun 9, 2181. [PubMed: 29872139]
4. Maniscalco JW, and Rinaman L (2018). Vagal interoceptive modulation of motivated behavior. Physiology (Bethesda) 33, 151–167. [PubMed: 29412062]
5. Han W, Tellez LA, Perkins MH, Perez IO, Qu T, Ferreira J, Ferreira TL, Quinn D, Liu ZW, Gao XB, et al. (2018). A neural circuit for gut-induced reward. Cell 175, 665–678.e23. [PubMed: 30245012]
6. Burdyga G, Varro A, Dimaline R, Thompson DG, and Dockray GJ (2006). Ghrelin receptors in rat and human nodose ganglia: putative role in regulating CB-1 and MCH receptor abundance. Am. J. Physiol. Gastrointest. Liver Physiol 290, G1289–G1297. [PubMed: 16423919]
7. Date Y, Murakami N, Toshinai K, Matsukura S, Niijima A, Matsuo H, Kangawa K, and Nakazato M (2002). The role of the gastric afferent vagal nerve in ghrelin-induced feeding and growth hormone secretion in rats. Gastroenterology 123, 1120–1128. [PubMed: 12360474]
8. Paulino G, Barbier de la Serre C, Knotts TA, Oort PJ, Newman JW, Adams SH, and Raybould HE (2009). Increased expression of receptors for orexigenic factors in nodose ganglion of diet-induced obese rats. Am. J. Physiol. Endocrinol. Metab 296, E898–E903. [PubMed: 19190260]
9. Sato M, Nakahara K, Miyazato M, Kangawa K, and Murakami N (2007). Regulation of GH secretagogue receptor gene expression in the rat nodose ganglion. J. Endocrinol 194, 41–46. [PubMed: 17592019]
10. Hayes MR, Moore RL, Shah SM, and Covasa M (2004). 5-HT3 receptors participate in CCK-induced suppression of food intake by delaying gastric emptying. Am. J. Physiol. Regul. Integr. Comp. Physiol 287, R817–R823. [PubMed: 15191908]
11. Schwartz GJ, and Moran TH (1994). CCK elicits and modulates vagal afferent activity arising from gastric and duodenal sites. Ann. N Y Acad. Sci 713, 121–128. [PubMed: 8185153]
12. Krieger JP, Langhans W, and Lee SJ (2015). Vagal mediation of GLP-1's effects on food intake and glycemia. Physiol. Behav 152 (Pt B), 372–380. [PubMed: 26048300]
13. Krieger JP, Arnold M, Pettersen KG, Lossel P, Langhans W, and Lee SJ (2016). Knockdown of GLP-1 receptors in vagal afferents affects normal food intake and glycemia. Diabetes 65, 34–43. [PubMed: 26470787]
14. de Lartigue G, Ronveaux CC, and Raybould HE (2014). Deletion of leptin signaling in vagal afferent neurons results in hyperphagia and obesity. Mol. Metab 3, 595–607. [PubMed: 25161883]
15. Clifton PG, Vickers SP, and Somerville EM (1998). Little and often: ingestive behavior patterns following hippocampal lesions in rats. Behav. Neurosci 112, 502–511. [PubMed: 9676968]

16. Hannapel R, Ramesh J, Ross A, LaLumiere RT, Roseberry AG, and Parent MB (2019). Postmeal optogenetic inhibition of dorsal or ventral hippocampal pyramidal neurons increases future intake. eNeuro 6, ENEURO.0457–18.2018.
17. Hannapel RC, Henderson YH, Nalloor R, Vazdarjanova A, and Parent MB (2017). Ventral hippocampal neurons inhibit postprandial energy intake. Hippocampus 27, 274–284. [PubMed: 28121049]
18. Henderson YO, Smith GP, and Parent MB (2013). Hippocampal neurons inhibit meal onset. Hippocampus 23, 100–107. [PubMed: 22927320]
19. Brunstrom JM, Burn JF, Sell NR, Collingwood JM, Rogers PJ, Wilkinson LL, Hinton EC, Maynard OM, and Ferriday D (2012). Episodic memory and appetite regulation in humans. PLoS ONE 7, e50707. [PubMed: 23227200]
20. Edwards A, and Abizaid A (2017). Clarifying the ghrelin system's ability to regulate feeding behaviours despite enigmatic spatial separation of the GHSR and its endogenous ligand. Int. J. Mol. Sci 18, 859.
21. Müller TD, Nogueiras R, Andermann ML, Andrews ZB, Anker SD, Argente J, Batterham RL, Benoit SC, Bowers CY, Broglio F, et al. (2015). Ghrelin. Mol. Metab 4, 437–460. [PubMed: 26042199]
22. Mani BK, Shankar K, and Zigman JM (2019). Ghrelin's relationship to blood glucose. Endocrinology 160, 1247–1261. [PubMed: 30874792]
23. Hsu TM, Suarez AN, and Kanoski SE (2016). Ghrelin: a link between memory and ingestive behavior. Physiol. Behav 162, 10–17. [PubMed: 27072509]
24. Suarez AN, Liu CM, Cortella AM, Noble EE, and Kanoski SE (2020). Ghrelin and orexin interact to increase meal size through a descending hippocampus to hindbrain signaling pathway. Biol. Psychiatry 87, 1001–1011. [PubMed: 31836175]
25. Drazen DL, Vahl TP, D'Alessio DA, Seeley RJ, and Woods SC (2006). Effects of a fixed meal pattern on ghrelin secretion: evidence for a learned response independent of nutrient status. Endocrinology 147, 23–30. [PubMed: 16179409]
26. Hsu TM, Hahn JD, Konanur VR, Noble EE, Suarez AN, Thai J, Nakamoto EM, and Kanoski SE (2015). Hippocampus ghrelin signaling mediates appetite through lateral hypothalamic orexin pathways. eLife 4, e11190. [PubMed: 26745307]
27. Arnold M, Mura A, Langhans W, and Geary N (2006). Gut vagal afferents are not necessary for the eating-stimulatory effect of intraperitoneally injected ghrelin in the rat. J. Neurosci 26, 11052–11060. [PubMed: 17065447]
28. Kentish SJ, Frisby CL, Kennaway DJ, Wittert GA, and Page AJ (2013). Circadian variation in gastric vagal afferent mechanosensitivity. J. Neurosci 33, 19238–19242. [PubMed: 24305819]
29. Kanoski SE, Rupprecht LE, Fortin SM, De Jonghe BC, and Hayes MR (2012). The role of nausea in food intake and body weight suppression by peripheral GLP-1 receptor agonists, exendin-4 and liraglutide. Neuropharmacology 62, 1916–1927. [PubMed: 22227019]
30. Moran TH, Baldessarini AR, Salorio CF, Lowery T, and Schwartz GJ (1997). Vagal afferent and efferent contributions to the inhibition of food intake by cholecystokinin. Am. J. Physiol 272, R1245–R1251. [PubMed: 9140026]
31. Williams DL, Kaplan JM, and Grill HJ (2000). The role of the dorsal vagal complex and the vagus nerve in feeding effects of melanocortin-3/4 receptor stimulation. Endocrinology 141, 1332–1337. [PubMed: 10746636]
32. Kanoski SE, Fortin SM, Arnold M, Grill HJ, and Hayes MR (2011). Peripheral and central GLP-1 receptor populations mediate the anorectic effects of peripherally administered GLP-1 receptor agonists, liraglutide and exendin-4. Endocrinology 152, 3103–3112. [PubMed: 21693680]
33. Ahmari N, Santisteban MM, Miller DR, Geis NM, Larkin R, Redler T, Denson H, Khoshbouei H, Baekey DM, Raizada MK, and Zubcevic J (2019). Elevated bone marrow sympathetic drive precedes systemic inflammation in angiotensin II hypertension. Am. J. Physiol. Heart Circ. Physiol 317, H279–H289. [PubMed: 31150271]
34. Zubcevic J, Jun JY, Kim S, Perez PD, Afzal A, Shan Z, Li W, Santisteban MM, Yuan W, Febo M, et al. (2014). Altered inflammatory response is associated with an impaired autonomic input to the

bone marrow in the spontaneously hypertensive rat. Hypertension 63, 542–550. [PubMed: 24366083]

35. Zubcevic J, and Potts JT (2010). Role of GABAergic neurones in the nucleus tractus solitarii in modulation of cardiovascular activity. Exp. Physiol 95, 909–918. [PubMed: 20591977]
36. Paton JF (1996). A working heart-brainstem preparation of the mouse. J. Neurosci. Methods 65, 63–68. [PubMed: 8815310]
37. Varga F, and Csáky TZ (1976). Changes in the blood supply of the gastrointestinal tract in rats with age. Pflugers Arch. 364, 129–133. [PubMed: 986621]
38. Geliebter A, Yahav EK, Gluck ME, and Hashim SA (2004). Gastric capacity, test meal intake, and appetitive hormones in binge eating disorder. Physiol. Behav 81, 735–740. [PubMed: 15234178]
39. Young A (2005). Inhibition of gastric emptying. Adv. Pharmacol 52, 99–121. [PubMed: 16492543]
40. Swanson LW (2018). Brain maps 4.0-Structure of the rat brain: an open access atlas with global nervous system nomenclature ontology and flatmaps. J. Comp. Neurol 526, 935–943. [PubMed: 29277900]
41. Davis EA, Zhou W, and Dailey MJ (2018). Evidence for a direct effect of the autonomic nervous system on intestinal epithelial stem cell proliferation. Physiol. Rep 6, e13745. [PubMed: 29932493]
42. Liu CM, Davis EA, Suarez AN, Wood RI, Noble EE, and Kanoski SE (2019). Sex differences and estrous influences on oxytocin control of food intake. Neuroscience. Published online November 15, 2019. 10.1016/j.neuroscience.2019.10.020.
43. Hsu TM, Konanur VR, Taing L, Usui R, Kayser BD, Goran MI, and Kanoski SE (2015). Effects of sucrose and high fructose corn syrup consumption on spatial memory function and hippocampal neuroinflammation in adolescent rats. Hippocampus 25, 227–239. [PubMed: 25242636]
44. Hsu TM, Hahn JD, Konanur VR, Lam A, and Kanoski SE (2015). Hippocampal GLP-1 receptors influence food intake, meal size, and effort-based responding for food through volume transmission. Neuropsychopharmacology 40, 327–337. [PubMed: 25035078]

Highlights

- Vagal afferent nerve (VAN) ghrelin signaling promotes hippocampal-dependent memory
- VAN ghrelin receptor (GHSR) knockdown disrupts meal patterns and metabolic indices
- VAN signaling is required for the hyperphagic effects of ghrelin in the dark cycle
- Gut-restricted circulating ghrelin increases VAN firing rate via VAN GHSR

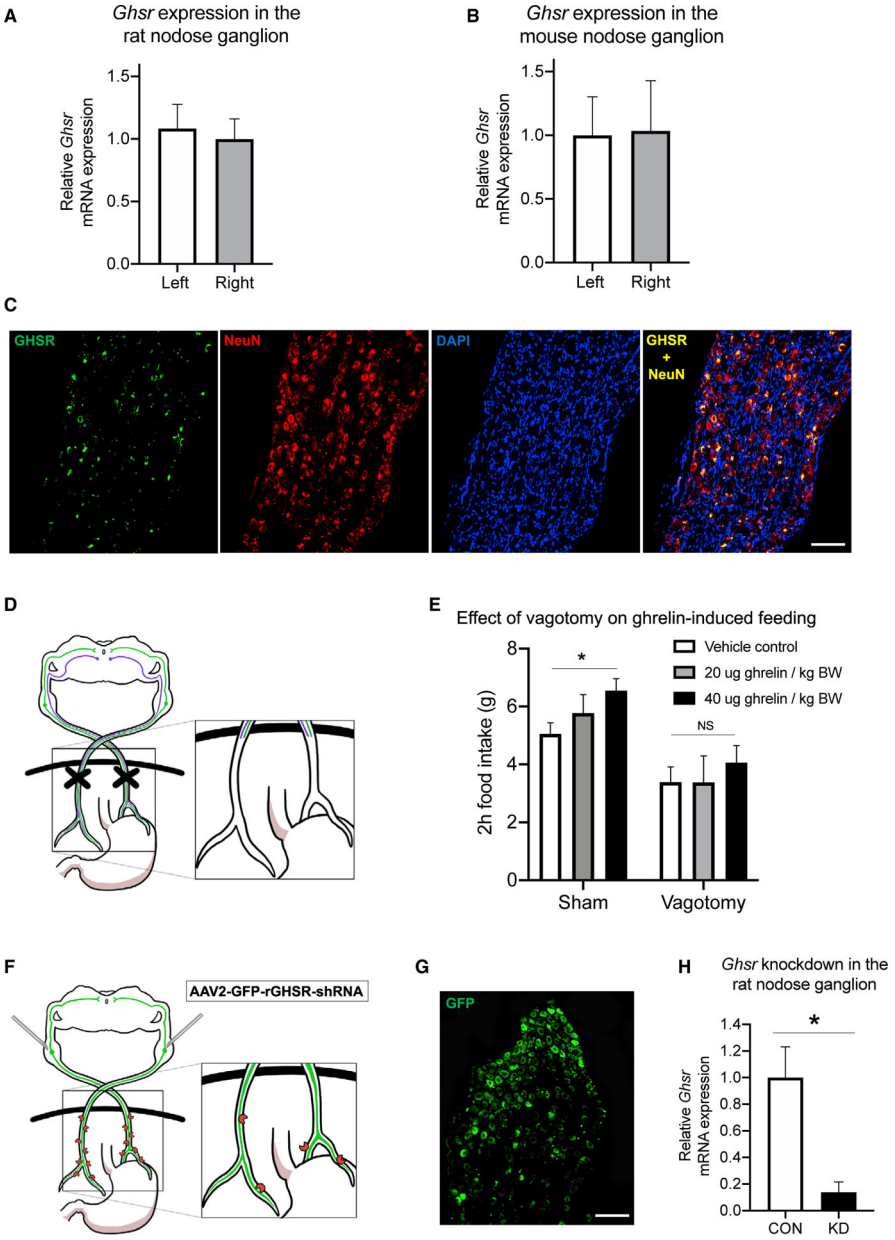

Figure 1. VAN Signaling Is Required for the Hyperphagic Effects of Peripheral Ghrelin, and the Ghrelin Receptor (GHSR) Is Expressed in the Nodose Ganglion and Is Reduced with Targeted RNAi

(A–C) The left and right nodose ganglia (LNG and RNG), which house VAN cell bodies, express *Ghsr* mRNA in both rats (A) and mice (B) with no differences in expression between LNG and RNG in either species. *Ghsr* mRNA (green) is exclusively expressed in rat nodose ganglion neurons (red, neuronal marker *NeuN*), as demonstrated by co-localization of *Ghsr* and *NeuN* (yellow), and approximately ~73% of *NeuN*+ nodose ganglion neurons co-express *Ghsr* (C).

(D and E) After complete bilateral subdiaphragmatic vagotomy in rats (D), the hyperphagic effect of i.p. ghrelin at 40 mg/kg BW injected in the early dark cycle was abolished

compared with controls (E; see also Figure S2 for comparison groups after saline injection when adjusted for body weight).

(F) VAN Ghsr expression is knocked down in rats via bilateral nodose ganglia injections of a custom-designed AAV (AAV-2 GFP-rGHSR-shRNA).

(G) Representative histology of VAN cell bodies in the nodose ganglion expressing the GHSR shRNA AAV with a green fluorescent protein (GFP) transgene.

(H) Gene expression analyses confirmed a statistically significant ~86% knockdown of the *Ghsr* gene in the nodose ganglion (see also Figure S3 for evaluation of Mch1r and Cb1r mRNA expression in the NG after GHSR knockdown).

All data presented as mean ± SEM.

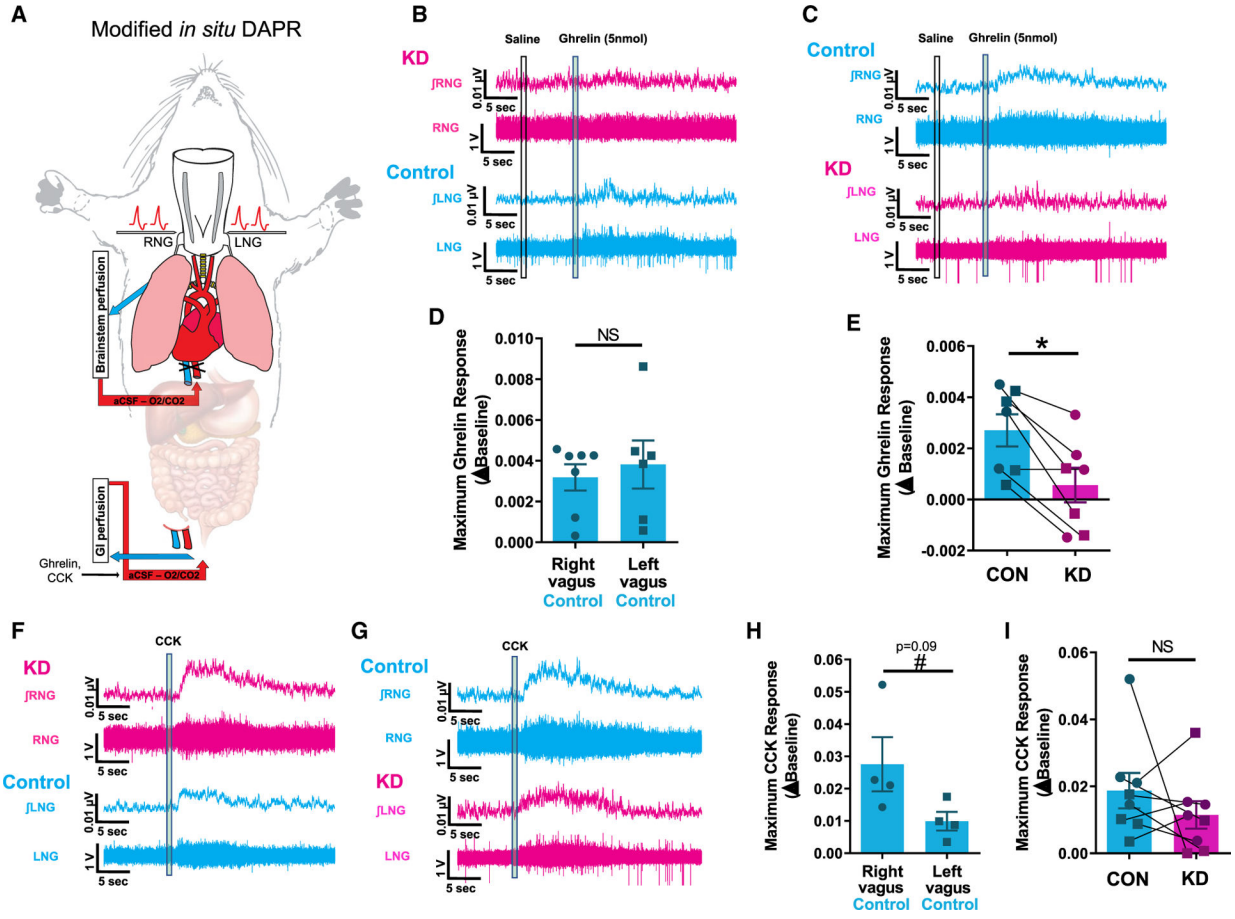

Figure 2. VAN-Specific GHSR Knockdown Blocks the VAN Neural Response to Gut-Restricted Ghrelin

(A) An *in situ* model of a decorticated artificially perfused rat (DAPR) was used to simultaneously record both left and right supranodose afferent activity in response to exogenous infusions of saline, ghrelin, or CCK restricted to the gastrointestinal circulation.

(B and C) Representative traces of right (top) and left (bottom) vagal afferent activity within the same animal in response to intra-arterial injection of ghrelin (5 nmol) (an animal with shRNA for GHSR in the RNG in B; an animal with shRNA for GHSR in the LNG in C). In the control AAV vagal side (cyan), ghrelin produces a small but reproducible and significant increase in vagal afferent activity, which is not present in the GHSR shRNA vagal side (magenta).

(D) There is no difference in maximum ghrelin response between control injected left or right vagal recordings.

(E) Conditional knockdown of ghrelin receptor significantly blunts ghrelin-induced vagal activity compared with control.

(F and G) Representative traces of right (top) and left (bottom) vagal afferent activity in response to intra-arterial injection of CCK (1 mg) within the same animal (an animal with shRNA for GHSR in the RNG in F; an animal with shRNA for GHSR in the LNG in G). CCK produces a pronounced increase in vagal afferent activity in both control and shRNA-injected sides.

(H) There is trend toward a greater maximum CCK response in the right compared to left vagus nerve ($n = 4$, $p = 0.09$).

(I) Knockdown of ghrelin receptor has no effect on CCK-induced vagal activity compared to control.

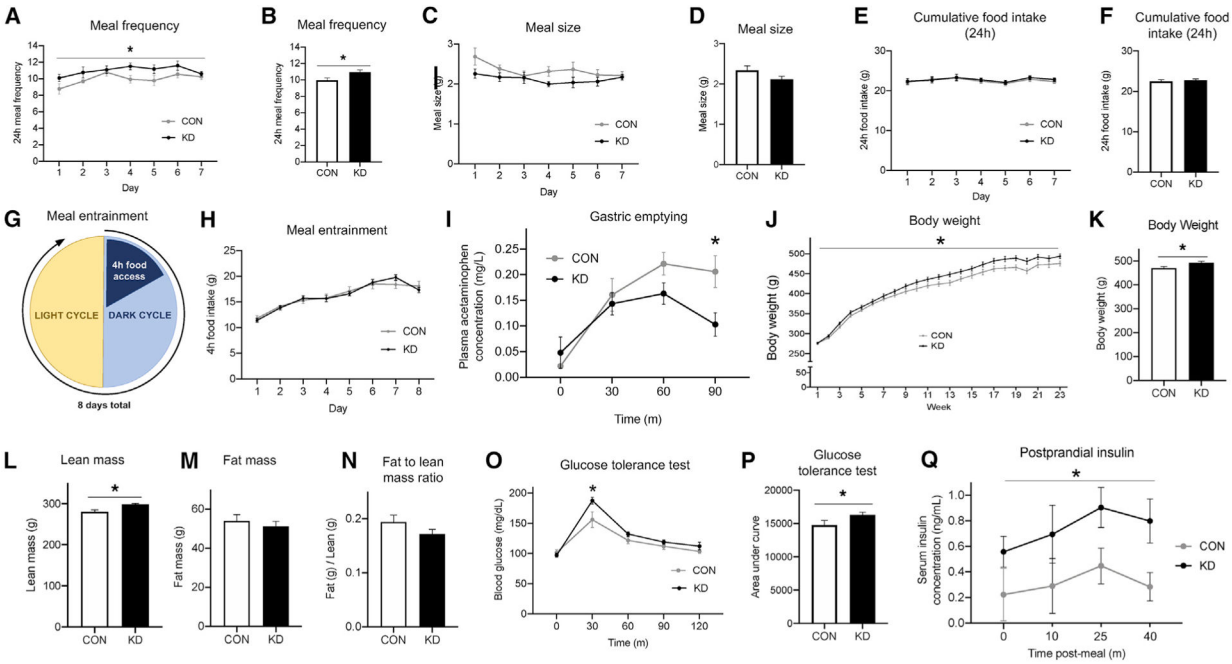

Figure 3. VAN-Specific GHSR Knockdown Increases Meal Frequency, Body Weight, and Lean Mass while Disrupting Gastric Emptying Rate and Peripheral Glucose Tolerance

(A–F) Compared with control animals, VAN-specific GHSR knockdown animals displayed an increased meal frequency (A and B) and a non-significant trend toward decreased meal size (C and D), such that there were no changes in 24 h cumulative food intake (E and F).

(G and H) Under meal entrainment conditions (G), there were no significant differences in food intake between knockdown and control animals (H).

(I) Rate of gastric emptying was significantly decreased in knockdown animals compared with controls 90 min after meal consumption.

(J–N) VAN-specific GHSR knockdown increased body weight compared with controls over time (J) and at 23 weeks post-surgery (K), at which point body composition was evaluated. Results showed increased lean mass in knockdown animals (L). However, there were no differences between groups in fat mass (M) or fat to lean mass ratio (N).

(O and P) VAN-specific GHSR knockdown impaired glucose tolerance compared with controls in an i.p. glucose tolerance test at the 30-min time point (O), and in total as measured by area under the curve (P).

(Q) VAN-specific GHSR knockdown postprandial increased serum insulin levels compared with controls.

All data presented as mean ± SEM.

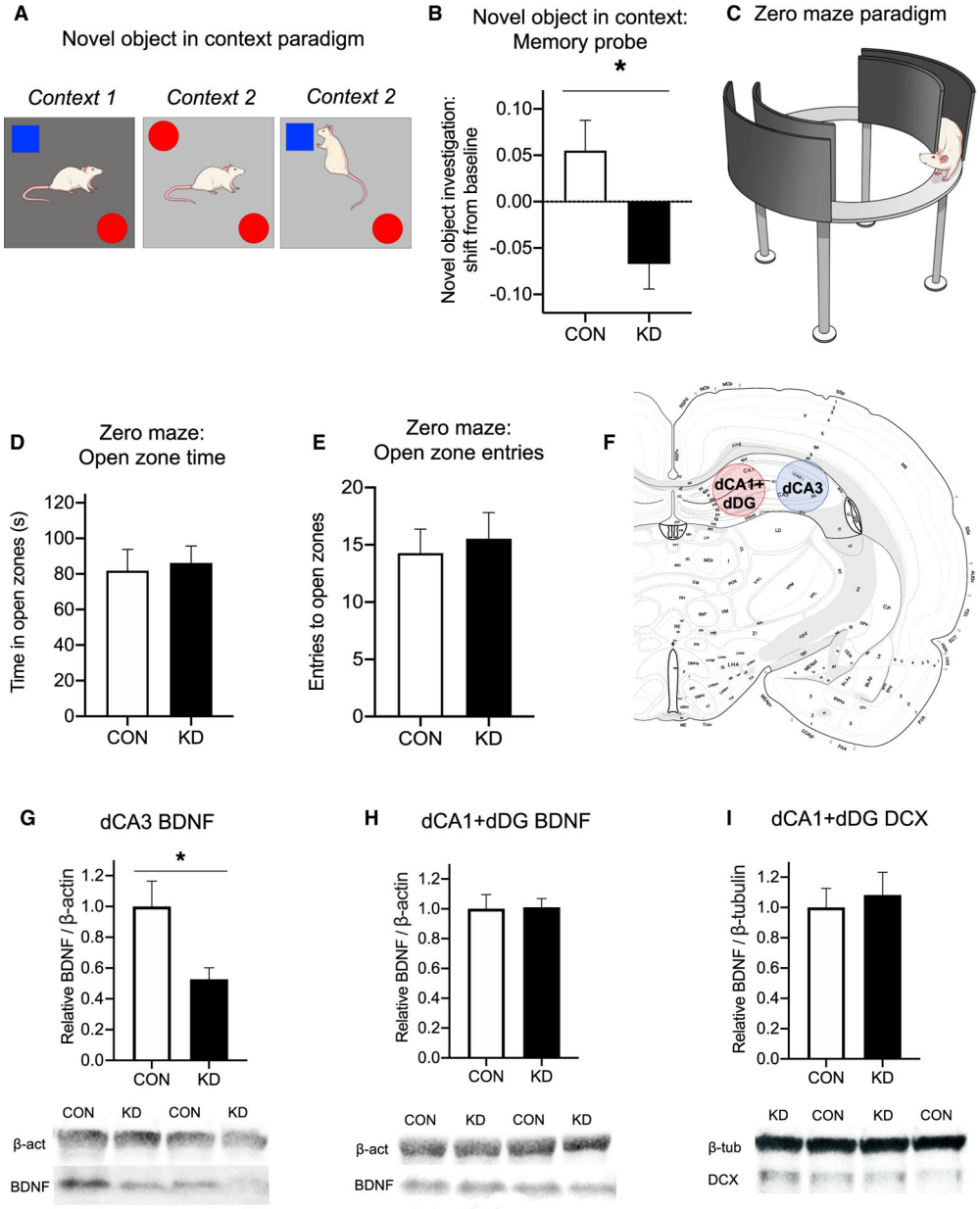

Figure 4. VAN-Specific GHSR Knockdown Impairs HPC-Dependent Contextual Episodic Memory and Reduces HPC CA3 BDNF without Affecting Anxiety-like Behavior

(A and B) In the novel object in context (NOIC) task (A), VAN-specific GHSR knockdown animals were significantly impaired in novel object exploration shift from baseline during the memory probe compared with controls (B), indicating that VAN-specific GHSR knockdown impairs HPC-dependent contextual episodic memory. (See also Figure S1 for effect of VAN GHSR knockdown on other types of memory.)

(C–E) In the zero maze task testing anxiety-like behavior (C), VAN-specific GHSR knockdown did not alter zero maze performance compared to controls, as measured by time in the open zones (D) and number of entries to open zones (E).

(F) Dorsal CA3 (dCA3) and dorsal CA1 plus and dorsal dentate gyrus (dCA1+dDG) lysates were analyzed for protein levels associated with neuroplasticity and neurogenesis.

(G and H) The neuroplasticity-associated protein BDNF was decreased in knockdown animals compared with controls in dCA3 lysates (G), but there were no differences between groups in dCA1+dDG lysates (H).

(I) There were no differences in the proliferation-associated protein DCX between groups in the dCA1+dDG lysate, where the proliferating dentate gyrus neurons are located.

KEY RESOURCES TABLE

REAGENT or RESOURCE	SOURCE	IDENTIFIER
Antibodies		
Rabbit anti-brain-derived neurotrophic factor (BDNF) antibody	Santa Cruz Biotechnology	Cat# sc-20981
Rabbit anti-β-actin antibody	Santa Cruz Biotechnology	Cat# NB600–503
Rabbit anti-doublecortin antibody	Abcam	Cat# ab18723
Rabbit anti-β-tubulin antibody	Cell Signaling	Cat# 2128S
Ghsr1a mRNA probe	Advanced Cell Diagnostics	Cat# 431991
NeuN mRNA probe	Advanced Cell Diagnostics	Cat# 436351-C2
Dapi mRNA probe	Advanced Cell Diagnostics	Cat# 323108
Rat *Ghsr* (growth hormone secretagogue receptor) TaqMan probe	Applied Biosystems	Rn00821417_m1
Rat *Mchr1* (melanin concentrating hormone receptor 1) TaqMan probe	Applied Biosystems	Rn00755896_m1
Rat *Cnr1* (cannabinoid receptor 1) TaqMan probe	Applied Biosystems	Rn00562880_m1
Rat *Gapdh* (Glyceraldehyde 3-phosphate dehydrogenase) TaqMan probe	Applied Biosystems	Rn01775763_g1
Mouse *Ghsr* (growth hormone secretagogue receptor) TaqMan probe	Applied Biosystems	Mm00616415_m1
Mouse *Gapdh* (Glyceraldehyde 3-phosphate dehydrogenase) TaqMan probe	Applied Biosystems	Mm99999915_g1
Bacterial and Virus Strains		
AAV2-GFP-U6-rGHSR-shRNA; shRNA sequence: CCGGACTGCAACCTGGTGTCCTTTGCTCGAGCAAGGACACCAGGTTGCAGTTTTTG	Vector Biolabs	www.vectorbiolabs.com
AAV2-GFP-U6-Scrmb-shRNA	Vector Biolabs	Cat# 7041
AAV-hSyn-ChR2(h134R)-eYFP	Addgene	Cat# 26973-AAV1
Chemicals, Peptides, and Recombinant Proteins		
TaqMan Fast Advanced Master Mix	Applied Biosystems	Cat# 4444557
TaqMan PreAmp Master Mix	ThermoFisher	Cat# 4391128
Ghrelin	Bachem	*Cat# 4033076*
Cholecystokinin (CCK-8)	Bachem	Cat# 4033010
Critical Commercial Assays		
RNeasy Lipid Tissue Mini Kit	Qiagen	Catalog # 74804
RNeasy Micro Kit	Qiagen	Catalog # 74004
QuantiTect Reverse Transcription Kit	Qiagen	Catalog # 205311
RNAscope® Fluorescent Multiplex Detection Reagent Kit	Advanced Cell Diagnostics	Catalog #320851
Rat Insulin ELISA	Crystal Chem Inc.	Cat #90010

REAGENT or RESOURCE	SOURCE	IDENTIFIER
Rat Acetaminophen ELISA	Cambridge Life Sciences	Cat# K8003
Deposited Data		
Data	This paper	https://osf.io/rufcz/
Experimental Models: Organisms/Strains		
Rat: Sprague Dawley (Outbred)	Charles River	N/A
Rat: Wistar (Outbred)	Envigo	N/A
Mouse: C57BL/6J	Jackson Labs	N/A
Rat: Sprague Dawley (Outbred)	Charles River	N/A